Journal of Coastal and Marine Engineering
Volume 1 • Number 1 • June 2018

SPH Modeling of Heave Motion Response of Pile-Supported Floating Breakwater

Kaveh Soleimani[1], Mohammad Javad Ketabdari[2]

1) Department of Marine Technology, Amirkabir University of Technology, Tehran, Iran, kv.soleimani@aut.ac.ir
2) Department of Marine Technology, Amirkabir University of Technology, Tehran, Iran, ketabdar@aut.ac.ir

Abstract: The interaction of sea waves and floating bodies is one of the pioneering fields of study in marine technology that has recently received a lot of attention. Floating breakwater can be an alternative for conventional breakwaters in anomalous conditions such as deep water, insufficient seabed and high sedimentation rates in typical wave climates where there is no need for full protection. In this article, the heave motion response of a single degree of freedom pile-supported floating breakwater was investigated employing WCSPH technique. To describe the momentum equation, the laminar viscous stress model, and to surmount the spurious pressure oscillation of the numerical technique, the Shepard density filter was employed. In addition, three different weighting functions including Gaussian, Cubic Spline and Quintic (Wendland) were compared to select the most appropriate one for modeling. The results showed that the Cubic Spline and Quintic weighting functions were more appropriate in navigating a solution for the problems with this kind of wave structure interaction. The velocity field near the FB showed that the maximum velocity of water particles occurred near the sharp edges of the body.

Keywords: Pile-Supported Floating Breakwater, Wave- Structure Interaction, WCSPH Method, Weighting Function.

1. Introduction

Most of the world's population lives in coastal areas. In these areas, marine activities such as fishing, sailing and marine leisure issues are prevalent. Therefore, there is an increasing demand for sheltered areas for marine vessels. The most common way of protecting harbors from the action of waves involves the use of different kind of breakwaters. Traditionally, rubble mound breakwaters are the most prevalent type for marina and harbor protection. However they are generally sea bottom seated massive structures, having huge weight to provide structural strength and stability against giant waves. Due to their trapezoidal shape, their construction cost increases with increase in water depth. This explains why the application of these structures is limited to shallow water depths. Additionally, these breakwaters reduce the circulation of water within the harbor and cut the littoral drift route. Consequently, application of these kinds of breakwaters induces an increase in pollution and sedimentation problems. In environmentally sensitive sites where there is no need for full protection, floating breakwaters can be considered as a feasible option. They are barriers located near the free surface where the energy flux is dominant. Their primary function is distortion of orbital motion of the water particles near the free surface, where the maximum amplitudes and velocities occur. These breakwaters do not have problems of water interchange, sedimentation or marine life mitigation. In addition, the cost of construction is mostly independent of the water depth. Floating breakwaters can be used in loose and mud covered sea bottom area. Due to precast and portability of floating breakwaters, they can be employed for temporary or seasonal protection.

Pile-supported floating breakwater is a type of floating breakwater that is allowed to rise and fall with waves, while being laterally restrained. Regularly, a pile-supported floating breakwater is a semi-fixed floating structure which is only free to move in heave direction.

There are few works on the interaction of waves with pile-supported floating breakwaters in the literature. Experimental studies on the interaction of waves with pile-supported floating breakwaters was conducted by Manuel (1997), Duclos et al., (2001), Ruol and Martinelli (2007, 2012) [1-4]. There are also some numerical investigations on this matter by Kim et al., (1994), Isaacson (1998), Koutandos et al., (2004), Diamantoulaki et al., (2008) [5-8].

Smoothed particle hydrodynamics is a meshless, lagrangian technique with good results in problems with free surface flows. In this research, this method was used for simulation of heave motion of a single degree of freedom pile-supported floating breakwater (FB). This research was conducted employing SPHysics, an open source FORTRAN code with the capability of modeling hydrodynamic problems with SPH meshless method.

To describe the momentum equation, the laminar viscous stress model was employed. To overcome the pressure oscillation of WCSPH technique, the Shepard density filter was used. Also, three different density filters were used. Additionally, three different weighting functions including Gaussian, Cubic Spline and Quintic (Wendland) were employed. Validation of the model results was performed using the experimental and numerical works of Ruol and Martinelli [3].

*Corresponding author.

2. Governing Equations

The conservation of continuity and momentum equations are the governing equations of compressible viscous fluid, which are represented as follows [9]:

$$\frac{1}{\rho}\frac{D\rho}{Dt} + \nabla.u = 0 \tag{1}$$

$$\frac{Du}{Dt} = -\frac{1}{\rho}\nabla P + g + \nu_0 \nabla.(\nabla u) \tag{2}$$

where ρ is the water density, u is the velocity vector, P is the pressure, g is the acceleration due to gravity and ν_0 is the kinematic viscosity. The laminar stress term is represented as follows [10]:

$$(\nu_0 \nabla^2 u)_a = \sum_b m_b \left(\frac{4\nu_0 \vec{r}_{ab} \nabla_a W_{ab}}{(\rho_a + \rho_b)\left|\vec{r}_{ab}\right|} \right) \vec{u}_{ab} \tag{3}$$

3. The SPH Concept

The SPH method is based on the integral interpolation theory. In this technique, the differential equations are converted to integral equations by employing an interpolation function. In fact, instead of physical properties, the local derivatives act on the interpolation function, which is an analytical function. Therefore, in SPH method, each function $A(r)$ is estimated by equation (4) [11]:

$$A(r) = \int A(r') W(r - r', h) dr' \tag{4}$$

where $W(r-r',h)$ is the weighting function and h is called the smoothing length. The performance of the SPH model is critically dependent on the choice of the weighting functions, since it determines how the variables are interpolated. The next step is the approximation of the function A from the integral form to the discrete form as follows:

$$A(r) = \sum_b m_b \frac{A_b}{\rho_b} W_{ab} \tag{5}$$

where the mass and density are denoted by m and ρ, respectively. W_{ab} is the weighting function or kernel.

In this research, three different kernel functions were employed:

Gaussian:

$$W(r,h) = \alpha_D \exp(-q^2) \tag{6}$$

Cubic Spline:

$$W(r,h) = \alpha_D \begin{cases} 1 - \frac{3}{2}q^2 + \frac{3}{4}q^3 & 0 \le q \le 1 \\ \frac{1}{4}(2-q)^3 & 1 \le q \le 2 \\ 0 & q \ge 2 \end{cases} \tag{7}$$

Quintic (Wendland):

$$W(r,h) = \alpha_D (1 - \frac{q}{2})^4 (2q+1) \quad 0 \le q \le 2 \tag{8}$$

where $\alpha_D = 1/\pi h^2$, $\alpha_D = 10/7\pi h^2$ and $\alpha_D = 7/4\pi h^2$ in Gaussian, Cubic Spline and Quintic kernels, respectively [12].

3.1. Equation of State

In WCSPH method, the fluid is treated as weakly compressible. To determine the fluid pressure, an equation of state is employed, which requires much less computational time than that of Poisson's equation in ISPH. The compressibility is adjusted to slow the speed of sound so that the time step in the model (using a Courant condition based on the speed of sound) is reasonable. Tait equation of state is defined as follows [13]:

$$P = B\left[\left(\frac{\rho}{\rho_0}\right)^{\gamma} - 1\right] \tag{9}$$

Where $B = c_0^2 \rho_0 / \gamma$ is the bulk modulus of elasticity of the fluid, c_0 is the speed of sound at reference density which is usually taken as the density of the fluid at the free surface ($\rho_0 = 1000 kg/m^3$) and $\gamma = 7$ is the polytropic constant. There is a speed of sound ($c_0^2 = \partial P / \partial \rho \mid \rho_0$) which is set by altering the value of B to be approximately 20 times that of the maximum fluid velocity.

3.2. Moving the Particles

Particles are moved according to the XPSH variant [14]:

$$\frac{dr_a}{dt} = v_a + \varepsilon \sum_b \frac{m_b}{\bar{\rho}_{ab}} v_{ba} W_{ab} \tag{10}$$

where $\bar{\rho}_{ab} = 0.5(\rho_a + \rho_b)$ and $\varepsilon = 0.5$. In this technique, the particle a is moved with a velocity that is close to the average velocity in its neighborhood.

3.3. Density Filter

Although the SPH simulations are generally robust, large fictitious pressure oscillations occurs in the particles pressure field. One of the computationally least expensive ways to surmount this challenge is to design a filter over the density of the particles and re-assign a density to each particle. There are two orders of correction, zeroth order and first order. In this research, a zeroth order density filter was used [12].

A quick and simple correction to the density field is the Shepard density filter:

$$\rho_a^{new} = \sum_b \rho_b W_{ab} \frac{m_b}{\rho_b} = \sum_b m_b W_{ab} \tag{11}$$

The kernel is corrected employing a zeroth order correction:

$$W_{ab} = \frac{m_b}{\sum_b W_{ab} \frac{m_b}{\rho_b}} \tag{12}$$

This filter is applied every 30 time steps.

3.4. Boundary Conditions

In this research, Monaghan boundary condition was employed. It was developed by Monaghan [15] to ensure that a water particle does not penetrates the solid boundary. Similar to the intermolecular forces, the boundary particles exert central forces on the fluid particles. In this approach, a water particle experiences a force f acting normal to the wall and is given by the following equation:

$$\vec{f} = \vec{n} R(\psi) P(\zeta) \varepsilon(z, u_\perp) \tag{13}$$

In this equation, $\vec{n}$ is the normal of the solid wall, ψ is the perpendicular distance of the particle from the wall, ζ is the projection of interpolation location ζ_i onto the chord connecting the two adjacent particles (the distance along the boundary of a fluid particle between two boundary particles) and $u_\perp$ is the velocity of the water particle projected onto the normal. The repulsion function, $R(\psi)$ is assessed using the normalized distance from the wall, $q = \psi / 2h$:

$$R(\psi) = A \frac{1}{\sqrt{q}} (1 - q) \tag{14}$$

where A is:

$$A = \frac{1}{h} 0.01 c_i^2 \tag{15}$$

c_i is the speed of sound corresponding to particle i .

Function $P(\zeta)$ is selected so that a water particle experiences a constant repulsive force as it travels parallel to the wall:

$$P(\zeta) = 0.5(1 + \cos(\frac{2\pi\zeta}{\Delta b})) \tag{16}$$

where Δb is the distance between any two adjacent boundary particles. The function $\varepsilon(z, u_\perp)$ is a modification to the Monaghan and Kos' original suggestion and modifies the magnitude of the force according to the local water depth and velocity of the water particle normal to the boundary:

$$\varepsilon(z, u_\perp) = \varepsilon(z) + \varepsilon(u_\perp) \tag{17}$$

where

$$\varepsilon(z) = \begin{Bmatrix} 0.02 & z \geq 0 \\ |z/h_0| + 0.02 & -h_0 \leq z < 0 \\ 1 & |z/h_0| > 1 \end{Bmatrix} \tag{18}$$

$$\varepsilon(u_\perp) = \begin{Bmatrix} 0 & u_\perp \geq 0 \\ |20u_\perp| / c_0 & |20u_\perp| < c_0 \\ 1 & |20u_\perp| > c_0 \end{Bmatrix} \tag{19}$$

Where z is the elevation above the local SWL, h_0 , $u_\perp = (\vec{v}_{WP} - \vec{v}_{BP}).\vec{n}$, WP and BP denotes the water particles and boundary particles, respectively and $c_0 = \sqrt{B\gamma/\rho_0}$ is the speed of sound at the reference density.

As seen in Figure 1, in a 2D situation, the boundary particle i is surrounded by $i-1$ and $i+1$ boundary particles and the tangential vector is given by $t = (\vec{r}_{i+1} - \vec{r}_{i-1}) / |\vec{r}_{i+1} - \vec{r}_{i-1}|$ so that the normal is found from $\vec{n}\vec{t} = 0$.

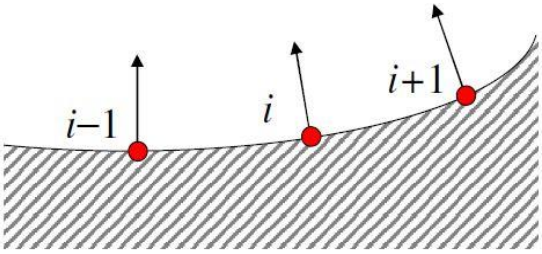

Figure 1. 2D particles and adjacent neighbors

3.5. Floating Objects

In SPH, a set of discrete boundary particles, which exert a repulsive force on the approaching water particles describe the boundary. Repulsive wall boundary particles exert a force on approaching water particles with a singularity in the force field as the interparticle distance approaches zero. The motion of a floating body is assessed by summing the contributions exerted on the boundary particles for an entire body. The force on each boundary particle is calculated by summing up the contribution from all the surrounding water particles within the surrounding kernel. Consequently, the boundary particle k experiences the following force per unit mass:

$$f_k = \sum_{a \in WPs} f_{ka} \tag{20}$$

where WPs denotes water particles and f_{ka} is the force per unit mass exerted by water particle a on boundary particle k . Using the principle of equal and opposite action and reaction, the force exerted by a water particle on each boundary particle is given by:

$$m_k f_{ka} = -m_a f_{ak} \tag{21}$$

Therefore, only repulsive force, f_{ak} exerted by the boundary particle k on water particle a is computed.

The equations of basic rigid body dynamics are used to determine the motion of the moving body, which in translational and rotational degrees of freedom are given by the following equations:

$$M\frac{dV}{dt}=\sum_{k\in BPs} m_k f_k \tag{22}$$

$$I\frac{d\Omega}{dt}=\sum_{k\in BPs} m_k (r_k-R_0)\times f_k \tag{23}$$

where M is the mass of the object, I is the moment of inertia, V is the velocity of object, Ω is the rotational velocity of the object, R_0 is the position of the center of mass and BPs denotes the boundary particles. These equations are integrated in time to predict the values of V and Ω for the beginning of the next time step. Each boundary particle that describes the moving body has the following velocity:

$$u_k = V + \Omega\times(r_k - R_0) \tag{24}$$

The boundary particles within the rigid body are then moved by integrating this equation in time domain.

3.6. Time Stepping Algorithm

In the absence of friction or viscous effects, Symplectic time integration schemes are time reversible [16]. Consequently, they are an attractive option for meshless particle schemes. First, the values of density and acceleration are calculated at the middle of the time step:

$$\begin{aligned}\rho_a^{n+1/2}&=\rho_a^n+\frac{\Delta t}{2}\frac{d\rho_a^n}{dt}\\ r_{-a}^{n+1/2}&=r_{-a}^n+\frac{\Delta t}{2}\frac{dr_{-a}^n}{dt}\end{aligned} \tag{25}$$

where n is the time step and $t = n.\Delta t$. Computation of the pressure $p_a^{n+1/2}$ is performed employing the equation of state. In the second step, the velocity and the position of the particles at the end of the time step is calculated using $d(\omega_i \rho_i v_{-i})/dt$:

$$\begin{aligned}(\omega_a\rho_a v_{-a})^{n+1}&=\omega_a\rho_a v_{-a}^{n+1/2}+\frac{\Delta t}{2}\frac{d(\omega_a\rho_a v_{-a})^{n+1/2}}{dt}\\ r_{-a}^{n+1}&=r_{-a}^{n+1/2}+\frac{\Delta t}{2}v_{-a}^{n+1}\end{aligned} \tag{26}$$

$d\rho_a^{n+1}/dt$ is computed at the end of the time step using updated values of v_{-a}^{n+1} and r_{-a}^{n+1} .

3.7. Variable Time Step

The control of the time step is dependent on the CFL condition, the forcing terms and the viscous diffusion term [14]. According to Monaghan and Kos [13], a variable time step is calculated using the equation:

$$\Delta t = \min(\Delta t_f, \Delta t_{cv}) \tag{27}$$

where

$$\begin{aligned}\Delta t_f &= \min_a\left(\sqrt{\frac{h}{|f_a|}}\right)\\ \Delta t_{cv} &= \min_a\left(\frac{h}{c_s+\max_b\left|\frac{h\vec{v}_{ab}\vec{r}_{ab}}{\vec{r}_{ab}^{\,2}}\right|}\right)\end{aligned} \tag{28}$$

Δt_f is based on the force per unit mass $|f_a|$ and Δt_{cv} combines the viscous and courant time step controls.

4. Validation

Dam-break flood waves are the most complex type of rapidly varied unsteady flows. It is a benchmark used as a standard test to verify numerical simulations and test the robustness and shock capturing capability of these models. In this section, the results of the dam-break benchmark test from SPH simulation were compared with experimental work of Issa [17]. The overall length and height of the water column was 30 cm, which was released from a channel of 90 cm length and 65 cm height. The released fluid impacts the front wall and its shape is changed. The aim of this test was to compare the progress of water column and its distortion due to impact on the wall in time domain. As can be seen from Figure 2 that SPH simulations have agreement with the experimental data. Therefore, the code has a good accuracy in modeling of hydrodynamic problems with large deformations.

5. Modeling

In this section, the results of the SPH simulation are presented. According to Ruol et al., [4], the choice of the most efficient restraining system of floating breakwater depends on the range of periods of interest and the ratio between draft and depth. In wave periods smaller than the natural period of oscillation and large drafts ($d/h > 0.2$), heave pile-supported floating breakwaters perform better than the other types.

To simulate the interaction of wave with the floating breakwater, a 2D model was employed. The set-up is composed of a breakwater with a length of 0.24 m, a height of 0.12 m and a draft of 0.06 m, which was located at a distance of 2 m from the wave maker. A sketch of the experimental set-up is shown in Figs.3-4. The wave height and period were 0.05 m and 0.87 s, respectively and was propagated in a water of 1.17 m depth. Since this wave was propagated in deep water, the flap type wave maker was employed for wave generation. The relationship between the wave height and wave maker stroke is as follows [18]:

$$\frac{H}{S}=4\left(\frac{\sinh kh}{kh}\right)\frac{kh\sinh kh-\cosh kh+1}{\sinh 2kh+2kh} \tag{29}$$

To set up the model, 216000 particles with a distance of 0.004 m in each direction were used. To describe the momentum equation, the laminar viscous stress model and to overcome the pressure oscillation, the Shepard density filter was employed. The results were compared with experimental and numerical studies of Ruol and Martinelli [3], which were based on the application of artificial viscosity (standard model). The generated wave, the

displacement and the velocity of the floating body are presented in Figures 5-7.

As can be seen from Figures 5 and 6, the best results were obtained from Cubic Spline and Wendland kernels, respectively. It should be noted that there was a phase lag between analytical and numerical waves, which was due to the wave maker effects. However, the amount of maximum wave profile and heave displacement was almost the same as the analytical and experimental results, respectively. Another point is that the total displacement of the body was about 5 cm, which was in the range of the wave height.

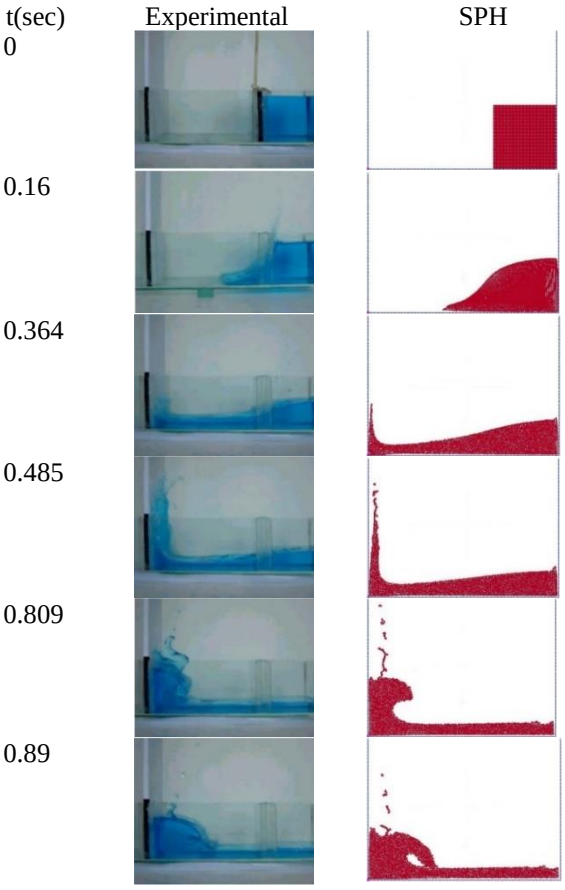

Figure 2. Dam-break test

Figure 3. Detail of pile connection in physical model test

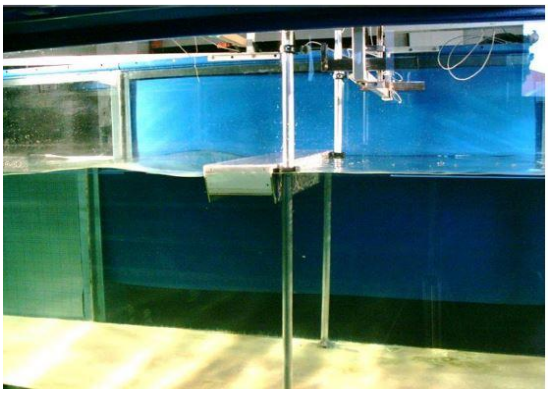

Figure 4. Piles installed in physical model test

Figure 8 shows different velocity fields (velocity magnitude, horizontal velocity field and vertical velocity field, respectively) at the time when the heave displacement is maximum. As evident in Figure 8, the maximum velocity magnitude of water particles occurred near the sharp edges of the floating body and its value was 0.44 m/s, which was more than twice of the maximum heave velocity of the floating object. It is expected that for a body with round edges, lower maximum water velocities occur. Additionally, it can be seen that the horizontal velocity of water particles has its maximum value at the bottom corners of the floating body. At this time, the vertical velocity of water particles at the bottom of the box is nearly zero, the same as the heave velocity of the floating body.

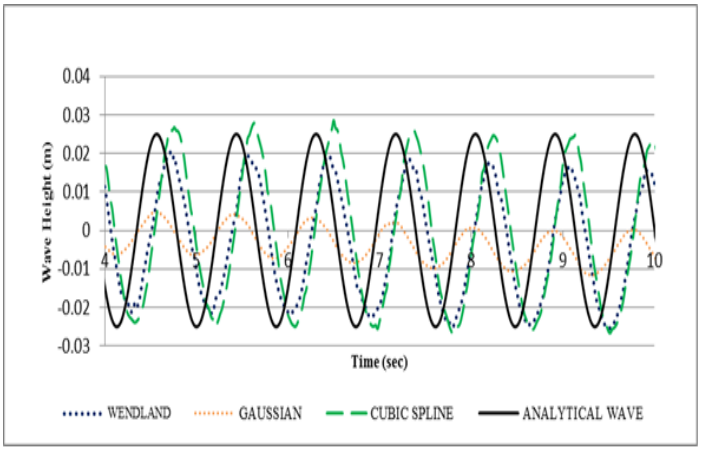

Figure 5. Accuracy of different kernels in the case of wave profile

6. Conclusion

In deep water conditions, construction of fixed breakwaters are costly, non – economical and require long construction time. Therefore, the use of floating breakwaters is recommended especially for short period waves. On the other hand, it is very important to obtain the motion response of these structures against waves. In this study, a 2D WCSPH code was employed to simulate the interaction of a linear wave with a pile-supported floating breakwater. To investigate the effect of the weighting function, three different kernel functions including Gaussian, Cubic Spline and Quintic were used.

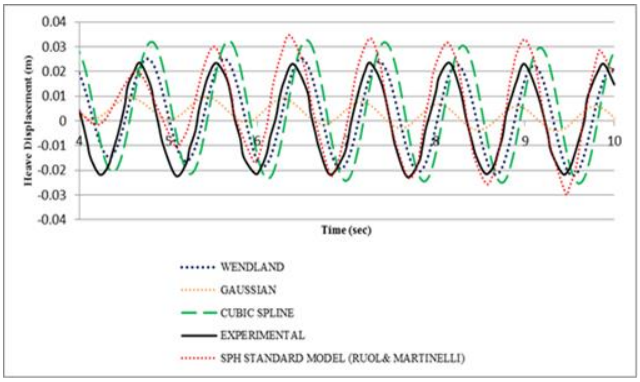

Figure 6. Accuracy of different kernels in the case of heave displacement of the floating body

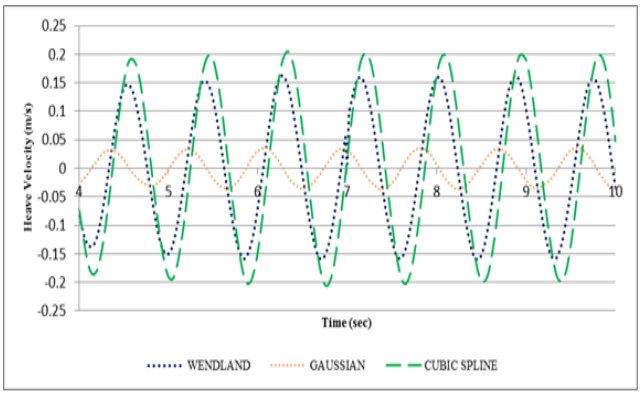

Figure 7. Comparison of results of different kernels in the case of heave velocity of the floating body

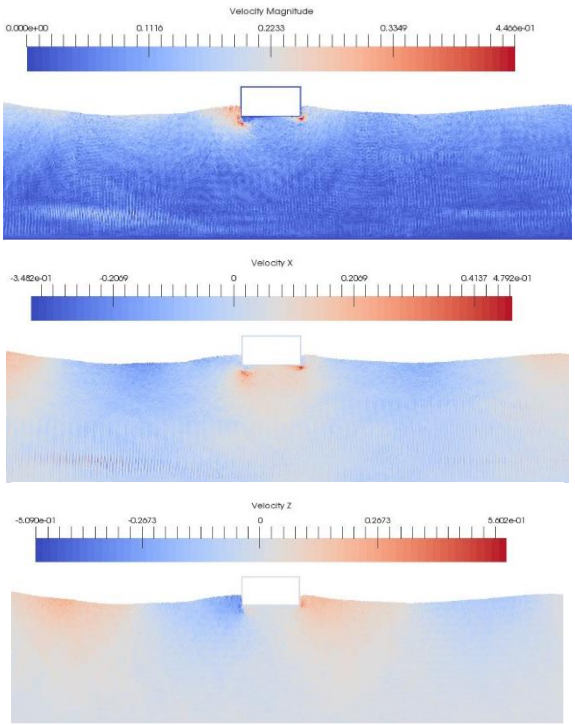

Figure 8. Different velocity fields when the heave movement is maximum

The results showed that the Cubic Spline and Quintic kernels were more suitable in simulating this problem. With these kernels, the results of the wave profile and heave displacement of the floating body were in good agreement with the analytical and experimental results, respectively. The results showed that the heave motion of the floating breakwater was nearly the same as the wave height. In addition, the maximum velocity of the floating body was less than half of the maximum wave orbital velocity, which occurred near the sharp edges of the floating body.

7. References

[1] Manuel, B., *Response of a Pile Restrained Floating Breakwater*, The University of British Columbia, Vancouver, Canada, MSc Thesis, 1997.

[2] Duclos, G., Clement, A.H., Gentaz, L. and Colmard, C., "Experimental and Numerical Study of a Half- Submerged Pile-Supported Breakwater", in *Proceedings The Eleventh International Offshore and Polar Engineering Conference*, Stavanger, Norway, June 17-22 2001, pp.221-228.

[3] Ruol, P., Martinelli, L., "Wave flume investigation on different mooring systems for floating breakwaters", *in Proceeding of Coastal Structures Conference*, Venice, Italy, July 2-4 2007, pp.327-338.

[4] Ruol, P., Martinelli, L., "Experimental And Numerical Investigation of the Effect of Mooring Stiffness on the Behaviour of P-Type Floating Breakwaters", *The Twenty-second International Offshore and Polar Engineering Conference*, Rhodes, Greece, June 17-22 2012.

[5] Kim, H.T., Sawaragi, T. and Aoki, S.I., Wave Control By Pile-Supported Floating Breakwaters, *The Foruth International Offshore and Polar Engineering Conference*, Osaka, Japan, April 10-15 1994.

[6] Isaacson, M., Baldwin, J., and Bhat, S., "Wave Propagation Past a Pile- Restrained Floating Breakwater", *International Journal of Offshore and Polar Engineering*, 8, 4, 1998, pp.265-269.

[7] Koutandos, E.V., Karambas, T.V. and Koutitas, C.G., "Floating Breakwater Response to Waves Action Using a Boussinesq Model Coupled with a 2DV Elliptic Solver", *Journal of Waterway, Port, Coastal and Ocean Engineering*, 130, 2004, pp. 243-255.

[8] Diamantoulaki, I., Angelides, D.C. and Manolis, G.D., "Performance of pile- restrained flexible floating breakwaters", *Applied Ocean Research*, 30, 2008, pp. 243-255.

[9] Varnousfaaderani, M.R. and Ketabdari, M.J., "Application of the modified weakly compressible SPH method to the 3D turbulent wave breaking impact", *Transactions of FAMENA*, 40, 2016, pp. 69-86.

[10] Lo, E.Y.M. and Shao, S., "Simulation of near-shore solitary wave mechanics by an incompressible SPH method", *Applied Ocean Research*, 24, 2002, pp. 275-286.

[11] Liu, G.R., Liu, M.B., *Smoothed Particle Hydrodynamics a meshfree method*, World Scientific Publishing Co, 2003.

[12] Gomez-Gesteira, M., Rogers,B.D., Crespo, A.J.C., "Dalrymple, R.A., Narayaswamy, M., SPHysics –development of a free-surface fluid solver – Part1: Theory", *Computers and Geosciences*, 48, 2012, pp. 289-299.

[13] Monaghan, J.J. and Kos, A., "Solitary Waves on a Cretan Beach", *Journal of Waterway, Port, Coastal and Ocean Engineering*, 125, 1999, pp. 145-154.

[14] Monaghan, J.J., "On the problem of penetration in particle methods", *Journal of Computational Physics*, 82, 1989, pp. 1-15.

[15] Monaghan, J.J., "Simulating free surface flows with SPH", Journal of Computational Physics, 110, 1994, pp. 399-406.

[16] Leimkuhler, B.J., Reich, S., and Skeel, R.D., *Integration Methods for Molecular dynamic, IMA Volume in Mathematics and its applications*, Springer, 1996.

[17] Issa, R., *Numerical assessment of the smoothed particle hydrodynamics gridless method for incompressible flows and its extension to turbulent flows*, University of Manchester, Manchester, United Kingdom, PhD Thesis, 2007.

[18] Dean, R.G., Dalrymple, R.A., *Water Wave Mechanics for Engineers and Scientists*, World Scientific Publishing Co, 2000.